

# ESFNet: Efficient Network for Building Extraction from High-Resolution Aerial Images

Jingbo Lin, Houbing Song, and Weipeng Jing

**Abstract**—Building footprint extraction from high-resolution aerial images is always an essential part of urban dynamic monitoring, planning and management. It has also been a challenging task in remote sensing research, due to complex environments and land cover objects in the high-resolution aerial images. In recent years, deep neural networks have made great achievement in improving accuracy of building extraction from remote sensing imagery. However, most of existing approaches usually requiring a large number of parameters and floating point operations for high accuracy, it leads to high memory consumption and low inference speed which are harmful to research. In this paper, we proposed a novel deep architecture named ESFNet which employs separable factorized residual block and utilizes the dilated convolutions, aiming to preserve slight accuracy loss with low computational cost and memory consumption. This is the first time introducing efficiency view of deep neural networks in remote sensing area. Our ESFNet is able to run at over 100 FPS on single Tesla V100, requires 6x less FLOPs and has 18x less parameters than state-of-the-art real-time architecture ERFNet while preserving similar accuracy without any additional context module, post-processing and pre-trained scheme. We evaluated our networks on WHU Building Dataset and compared it with other state-of-the-art architectures. The result and comprehensive analysis show that our networks are benefit to efficient remote sensing researches and applications, and can further extended to other areas. The code is public available at: <https://github.com/mrluin/ESFNet-Pytorch>

**Index Terms**—Remote Sensing, Building Extraction, Deep Learning, Efficient Neural Networks, Low Computational Cost, Low Memory Consumption

## I. INTRODUCTION

High-resolution aerial images are widely used in modern smart cities, one of the most import applications is automatic building extraction (shown in Fig. 1) which is aimed to separate pixels belong to buildings with others in complex

This paragraph of the first footnote will contain the date on which you submitted your paper for review. It will also contain support information, including sponsor and financial support acknowledgment. For example, “This work was supported in part by the U.S. Department of Commerce under Grant BS123456.”

The next few paragraphs should contain the authors’ current affiliations, including current address and e-mail. For example, F. A. Author is with the National Institute of Standards and Technology, Boulder, CO 80305 USA (e-mail: author@ boulder.nist.gov).

S. B. Author, Jr., was with Rice University, Houston, TX 77005 USA. He is now with the Department of Physics, Colorado State University, Fort Collins, CO 80523 USA (e-mail: author@lamar.colostate.edu).

T. C. Author is with the Electrical Engineering Department, University of Colorado, Boulder, CO 80309 USA, on leave from the National Research Institute for Metals, Tsukuba, Japan (e-mail: author@nrim.go.jp).



Fig. 1. The example of building extraction tasks from aerial images. (a) is the original high-resolution aerial images and (b) is related ground truth, the buildings are in white and others in black. (c) is the segmentation result of the network we proposed.

urban environments, and it can be considered as dense pixel-level classification problem, also defined as semantic segmentation task in computer vision. Semantic segmentation of remote sensing imagery has great significance on remote sensing research and applications including sea-land segmentation [1], automatic road detection [2], and complex land cover objects classification [3].

Nowadays, the remote sensing technology has reached an unprecedented level, the advanced sensors can provide more and more high-quality, high-resolution aerial images with much higher ground sampling distance than the past [4], so that the imagery usually contains abundant land cover information and confusing environment backgrounds specifically in modern cities, which increased the difficulty on semantic segmentation task in urban areas. As a result, traditional learning-based method, which is over dependent upon manual designed features, cannot solve the problems of large scale dataset and meet requirements of nowadays practical applications.

In the last several years, convolutional neural networks have made great achievement in a variety of computer vision tasks, such as classification [5], object detection [6], semantic segmentation [7] and so on. It has also exhibited its powerful feature extraction capability in remote sensing area compared to traditional methods. Since the milestone work of Long *et al.* [8], converts the classical CNN architecture to fully convolutional neural network (FCN) which replaces the fully

connected layers into intermediary score maps and uses multi-scale feature fusion scheme to solve the dense pixel-level classification problem in 2014, the deep neural networks approaches have been extensively used in building extraction and other semantic segmentation tasks, gradually replacing the conventional approaches in which features are extracted manually. Benefit from the structure of FCN, researchers extended FCN-like architectures into encoder-decoder architectures and using long-range connections for feature fusion, such as SegNet [9], DeconvNet [10] and U-Net [11], to name a few. Encoder is usually based on fashion classification architectures and designed to get high-level semantic representation of the whole imagery, and the decoder is used to recover the resolution of the high-level feature maps to the original imagery size, because the high-level feature maps are in small size and downsampled in encoder phase, For further improving accuracy, deeplab family [12, 13, 14, 15] achieve it by using post-processing and additional expressive module, such as dense conditional random fields (dense-CRF) [12] and atrous spatial parallel pyramid (ASPP) [14, 15]. These networks significantly improved segmentation accuracy, though usually requires high computational cost, large memory consumption and too much time to train. It is not efficient for scientific research specifically in remote sensing research which also needs large memory allocation for data loading with constraint computational resources. So besides accuracy, computation complexity, memory usage of models and inference speed are also essential metrics to measure the performance of architecture [16]. Under this intuition, there is a variety of architectures are designed towards light-weight and low computational cost while preserving state-of-the-art accuracy, such as MobileNet family [17, 18], ShuffleNet family [16, 19], ENet [20], ERFNet [21], EDANet [22] and so on. The trade-off between speed and accuracy becomes a key element for designing these efficient architectures.

As far as we know this is the first time introducing the efficiency view of deep neural networks in remote sensing research, specifically in building extraction task. Inspired by factorized residual block in real-time architecture ENet [20] and ERFNet [21], we proposed highly improved architecture called Efficient Separable Factorized Network (ESFNet). Benefits from depth-wise convolutions we employ separable factorized residual block (SFRB) module as our core module, it can compress model size significantly and drastically reduce the computation complexity. Furthermore, we extended our model to ERFNet-mini-ex based on the characteristics of ResNet [23] and the factors that influence the efficiency of networks for semantic segmentation tasks, and the ESFNet-mini-ex performs much better than the base in speed. Then we evaluated our architecture on a recent expressive building dataset, WHU Building Dataset, via comparing with other state-of-the-art networks and comprehensive analysis, elaborating that our model is an efficient backbone for semantic segmentation tasks and the idea can be further extended to other computer vision tasks.

In summary, there are three main contributions of this work, and highlighted as follows.

- 1) We proposed a novel efficient network named ESFNet, which employs separable factorized residual block with dilated convolutions. It can run 100.29 FPS on single Tesla V100 and achieve 85.34% IoU on WHU Building Dataset which is similar to the state-of-the-art networks, our ESFNet-mini-ex further improves the inference speed to 142.98 FPS and achieves 84.57% IoU that keeps a slight accuracy loss.
- 2) The proposed ESFNet requires 6x less floating point operations, 18x less parameters and can run 12 more frames per second than novel real-time architecture ERFNet, only has 2% accuracy loss which can be considered as a proper trade-off between accuracy and efficiency. Our ESFNet-mini-ex can be better that performs 54 more frames per second with 3% accuracy loss.
- 3) We designed comprehensive ablation studies to observe the performance of different designation and analyze the reasons behind them.

The rest of the paper is organized as follows. In Section II we review related works and the differences from ours. In Section III A we introduce the core module we proposed and Section III B shows detailed information of our whole model. The Section IV exhibits comprehensive experiment result and analysis. Section V concludes this paper.

## II. RELATED WORKS

In this section we will quickly review the existing works about semantic segmentation tasks in remote sensing research especially in building extraction. Since FCN architecture was proposed, there emerged lots of FCN-based methods, variants of FCN-structure used in semantic segmentation and achieved high accuracy than traditional methods. But it means to pay the equivalent price for the high accuracy. The existing works usually ignore the efficiency of the architecture, as a result most of state-of-the-art models usually have heavy-weight structures which is harmful for the cases with constraint computational resources. So in the following part we discuss from high-accuracy networks, high-efficiency networks and novel efficient modules to express our original intention.

### A. High Accuracy Architecture

Following the structure of FCN [8], most of recent building extraction studies are benefit from FCN-based methods. Maggiore *et al.* [24] designed a multi-scale neuron module in order to reduce the trade-off between recognition and localization, but there are lots of large kernel in their network, such as  $8 \times 8$  and  $9 \times 9$ . The large kernel bring large amount of parameters and high memory consumption, and it is proved to be inefficient and can be replaced by stacking  $3 \times 3$  kernels in [25] while preserving the same receptive field. Yuan [26] tackled pixel-wise prediction by integrating activation from multiple layers in different stages, but the VGG-based straight up and down structure is not benefit for information flow and feature reuse. Inspired by Ronneberger *et al.* [11], another popular architecture extensively used in segmentation tasks is

encoder-decoder structure and it is first used in biomedical. Li *et al.* [27] proposed encoder-decoder architecture and employed Dense-block [28] as their core module which can improve representation capability of the network but needs high computational cost and memory allocation. Ji *et al.* [29] proposed Siamese U-Net to improve segmentation performance by multi-scale input, but the deep symmetry architecture means it needs heavy-weight decoder which leads to high memory consumption and low inference speed. As a result, although all the networks mentioned above make great success on accuracy, they are not suitable for practical applications and efficient remote sensing research.

### B. High Efficiency Architecture

Some methods to obtain small-size networks are shrinking, factorizing or compressing pre-trained networks [17]. Another completely different method for obtaining efficient and small networks is utilizing efficient network architecture, such as residual block, kernel factorization and depth-wise convolutions. ENet [20] is one of the first networks designed towards light-weight architecture, it benefits from ResNet [23] structure and factorized kernel to keep low computational cost, furthermore it provides principles of building efficient segmentation networks. An extension of ENet [20], ERFNet [21] also benefits from residual block and factorized kernel, and get much better balance between accuracy and efficiency. EDANet [22] employs asymmetric residual structure with dilated convolutions and the dense connectivity to achieve high efficiency. Recent works such as BiSeNet [30] and ICNet [31] also have a better trade-off between accuracy and performance, but they are not easy to deploy and difficult in migrating to other tasks and areas due to their complex structures. From the above, most of recent novel real-time segmentation networks are benefit from residual learning and kernel factorization, and there is still a big room for further improvement.

### C. Novel Efficient Modules

Most of existing efficient networks are benefit from two aspects, that are efficient convolution operation and efficient structure. Group convolution [32] is an efficient convolution operation and widely used in many efficient networks, it divides the input feature maps into some independent groups and kernels of each group share the same weight in order to reduce the number of parameters. Depth-wise convolution is extreme case of group convolution, in which the number of groups is equal to input channels. One of the most popular efficient network MobileNet [17], it replaces the standard convolution into depth-wise one following by point-wise one, but the point-wise convolution costs so much, and then it is replaced by channel shuffle operation in ShuffleNet [19] in order to reduce the heavy burden. Residual learning structure is an efficient structure and it is extensively used in recent novel real-time networks [20, 21, 22, 30]. It is conducive to information flow in the networks and it can speed up the training phase. Additionally, it also mitigates the degradation problem of the deep neural networks.

In this paper, our ESFNet adopts the factorized bottleneck residual blocks to highly reduce the parameters and computational cost, we also introduced the novel depth-wise separable convolutions into our core module for further improving efficiency of the network. Utilizing characteristics of ResNet [23] structure, we explored on our model and proposed ESFNet-mini-ex which performs much better. Our ESFNet only requires small amount of parameters, low memory consumption but high inference speed while preserving similar accuracy to the state-of-the-art.

## III. PROPOSED METHODS

In this section, we first have an overview on our efficient architecture. In subsection A, we explain the core module separable factorized residual block (SFRB) in detail, and analyze the designation reasons behind it. In subsection B, we further elaborate other parts of our network.

TABLE I  
THE DETAILED INFORMATION OF OUR PROPOSED NETWORK ESFNET, WHERE “SFRB” IS OUR CORE MODULE, SEPARABLE FATORIZED RESIDUAL BLOCK. AND THE INPUT AND OURPUT ARE IN HXC FORMAT, WHERE H IS SPATIAL SIZE AND C IS NUMBER OF CHANNEL OF THE FEATURE MAPS.

	ID	Blocks	Input	Output
Encoder	1	Initial Block	512x3	256x16
	2	Down Sampling Block	256x16	128x64
	3-7	5 x SFRB (dilation rate 1)	128x64	128x64
	8	Down Sampling Block	128x64	64x128
	9	SFRB (dilation rate 1)	64x128	64x128
	10	SFRB (dilation rate 2)	64x128	64x128
	11	SFRB (dilation rate 1)	64x128	64x128
	12	SFRB (dilation rate 4)	64x128	64x128
	13	SFRB (dilation rate 1)	64x128	64x128
	14	SFRB (dilation rate 8)	64x128	64x128
	15	SFRB (dilation rate 1)	64x128	64x128
	16	SFRB (dilation rate 16)	64x128	64x128
	17	Transposed_conv2d (s=2)	64x128	128x64
	18	SFRB (dilation rate 1)	128x64	128x64
	19	SFRB (dilation rate 1)	128x64	128x64
Decoder	20	Transposed_conv2d (s=2)	128x64	256x16
	21	SFRB (dilation rate 1)	256x16	256x16
	22	SFRB (dilation rate 1)	256x16	256x16
	23	Transposed_conv2d (s=2)	256x16	512x2

The detailed network architecture of ESFNet is shown in Table I, the whole framework is encoder-decoder structure similar to most of segmentation networks. It consists of three down sampling blocks, two stages which have 5 SFRB and 8 SFRB respectively and a light-weight decoder following the principle of ENet [20]. The ESFNet achieves high performance with low computational cost and memory consumption without any other context modules, post-processing and additional scheme.

### A. Our Core Module

Separable factorized residual block (SFRB) is our core module as shown in Fig. 2(a), which introduces depth-wise separable convolution into novel efficient factorized residual block and incorporates with dilated convolutions in order to keep large receptive field with small down sampling rate, so

that avoiding the loss of unrecoverable spatial information. In the following part, we will discuss each component of our SFRB.

### 1) Depth-wise Separable Convolutions

The depth-wise separable convolution is considered as key-module in novel efficient networks [16, 17, 18, 19], it split the full convolution operations into two independent operations, depth-wise convolution and point-wise convolution. In depth-wise convolution, the number of groups is equal to the number of input feature maps, it means each kernel has single feature map in and single feature map out and these kernels share weight with each other in order to reduce parameters. Point-wise convolution is standard convolution with  $1 \times 1$  kernel size, aiming to combine the channel-wise independently features from depth-wise convolution. Thus the standard convolution can be changed into the combination of depth-wise convolution following by point-wise convolution, and it drastically reduces the model size leading to low computation cost and memory consumption.

For further explanation, we take  $C_{in} \times H \times W$  as size of input feature map and output size is  $C_{out} \times H \times W$  where  $C_{in}$  and  $C_{out}$  is the number of input channel and output channel respectively,  $H$  and  $W$  is spatial size of feature map, and the kernel size is  $K$ .

Therefore, the floating point operations (FLOPs) and the number of parameters needed of a standard convolution can be computed as:

$$K \times K \times H \times W \times C_{in} \times C_{out} \quad (1)$$

$$K \times K \times C_{in} \times C_{out} \quad (2)$$

And the FLOPs and the number of parameters of depth-wise separable convolutions are:

$$K \times K \times H \times W \times C_{in} + H \times W \times C_{in} \times C_{out} \quad (3)$$

$$K \times K \times C_{in} + C_{in} \times C_{out} \quad (4)$$

For simplicity, the kernel size  $K$  is 3,  $C_{in}$  and  $C_{out}$  are both equal to  $C$ ,  $H$  and  $W$  are equal to  $M$ . Using (1) and (2), (3) and (4) we calculate that there is about 9x reduction in FLOPs and the number of parameters (model size). Further combined with factorized convolution which we will discuss in the next part, it can achieve greatly improvement on efficiency of networks.

### 2) Factorized Convolutions

If the depth-wise separable convolutions decompose the standard convolutions in stage-wise as described above, then the Factorized convolutions decompose the standard convolutions in kernel-wise. As Alvarez *et al.* [33] has proved that, each ND kernels can be decomposed into N consecutive layers of 1D kernel. Here we only consider the 2D kernels, and it is easy to convert the situation to ND kernels. Standard 2D convolutions with  $K \times K$  kernels, where  $K$  is kernel size, can be converted to two 1D convolutions with  $K \times 1$  kernel size and  $1 \times K$  kernel size. On one hand the factorized convolutions downsize the model by reducing redundant parameters; on the other hand, it also plays a role of regularizer

in the whole network that enhances generalizing capability of model.

Continue with the analysis above, the FLOPs and parameters needed for factorized convolutions are:

$$2 \times K \times M \times M \times C \times C \quad (5)$$

$$2 \times K \times C \times C \quad (6)$$

And it is 3x less than the standard one. When incorporating with depth-wise separable convolutions, the computation and memory cost further highly reduce:

$$2 \times K \times M \times M \times C + M \times M \times C \times C \quad (7)$$

$$2 \times K \times C + C \times C \quad (8)$$

There are  $3 \times M \times M \times C$  fewer FLOPs and  $3 \times C$  less parameters than the original separable one, and it is another great improvement upon convolution operation especially when the feature maps have large spatial size and amounts of channels.

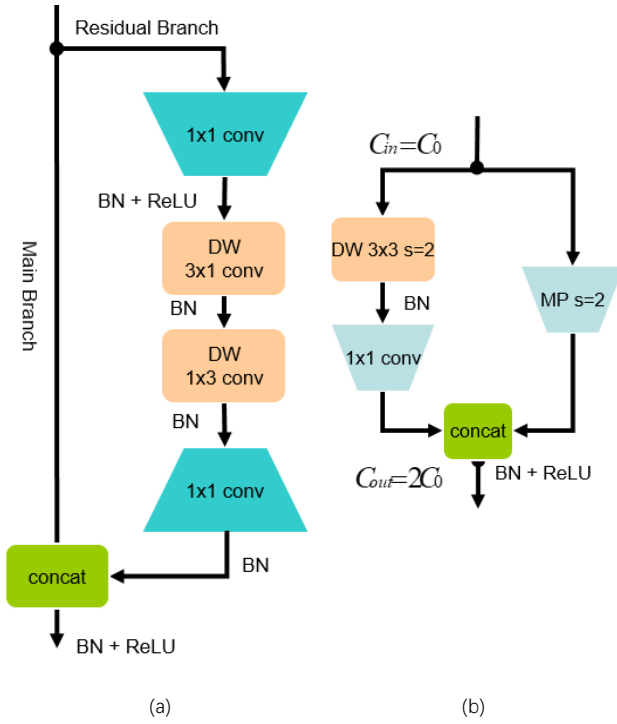


Fig. 2. Detailed description of our core module SFRB (a) and our improved down sampler (b). “concat” means concatenation operation, “MP” is Map Pooling down sampling layer and “s” means the stride of layer.

### 3) Dilated Convolutions and Receptive Field

In order to classify fine grid categories in high-resolution aerial images, the models usually need to have large receptive field (RF) [34] that can lead to rich context information for each pixel (cover the most area of high-resolution images). The method used in the past to enlarge receptive field is stacking convolution layers and down sampling layers, but too much convolution layers brings large burden of computation and memory, in addition over down sampling is harmful to dense pixel-level classification, due to the loss of unrecoverable spatial information. We evaluate 8x down sampling and 16x down sampling with the same architecture on WHU Building Dataset, the prediction of 16x down sampling network is really

bad than 8x one, it indicates the spatial information is equally important with context information in dense classification tasks. Contrast to the previous methods, dilated convolutions can enlarge receptive field without additional parameters increase, it implemented by inserting  $R-1$  zeros between two consecutive kernel values along each dimension [34, 35], where  $R$  is dilation rate. Additionally, we define  $RF_0 = 0$  and  $FeatureStride_0 = 1$ , then the receptive field of pixels in each layer can be calculated by:

$$FeatureStride_l = \prod_{i=1}^l stride_i \quad (9)$$

$$RF_l = RF_0 + \sum_{i=1}^l (K_i - 1) \times FeatureStride_{i-1} \times R_i \quad (10)$$

Where  $RF_i$ ,  $K_i$ ,  $R_i$  and  $stride_i$  are the receptive field, kernel size, dilation rate and stride of the  $i$ th layer respectively. Inspired by [34] and other novel networks [14, 36], the dilation rate is usually set to sequence and we set dilated convolutions in stage2 demonstrated (shown in Table I), and the sequence of dilation rate is 1, 2, 1, 4, 1, 8, 1, 16. Using (9) and (10), we can calculate the receptive field of our ESFNet is 599, and if we remove the dilated convolutions in stage2, the receptive field is only 183 that cannot cover most area of the image. What the disadvantage is, the dilated convolutions make networks need to keep much high-resolution feature maps in the intermediary layers, which usually leads to high memory cost [37].

#### 4) Bottleneck or Non-bottleneck

The basic idea of ResNet is to reduce degradation problem present in architectures that stacking large amounts of layers [23]. There are two implementations of residual block, the bottleneck structure and non-bottleneck structure. The previous works [38] reported that non-bottleneck layers gain more accuracy from increased depth than the bottleneck one, and it indicates that the bottleneck design still struggles with degradation problem. There is only around 1% accuracy gap between the same network with non-bottleneck structure and bottleneck structure in our experiments, but the bottleneck one requires less parameters and lower computational complexity as shown in Table II. This can be seen it does not suffer from the degradation problem, and the purpose of our work is to design efficient network with as low a memory footprint and computational cost as possible, so we choose bottleneck residual structure as our residual block backbone. The detailed information of different structures is concluded in Table II

As Fig. 2(a) demonstrates that, in residual branch the first standard  $1 \times 1$  convolutional layer is used to compress input feature maps into 4x less, following by two depth-wise factorized convolution instead of the standard  $3 \times 3$  convolution in original work [23] and the compressed feature maps are recovered by the last  $1 \times 1$  convolutional layer. Note that we use batch normalization [39] and ReLU [40] non-linear function after each convolutional layers, but no ReLU after depth-wise separable convolutions [18, 41] and the  $1 \times 1$  convolutions which used for recovering.

#### B. Network Design

In this subsection, we discuss from down sampling block and decoder which are equally important.

TABLE II

DETAILED INFORMATION OF DIFFERENT RESIDUAL STRUCTURES. WHERE “BT” = BOTTLENECK STRUCTURE, “FAC” = FACTORIZED CONVOLUTIONS, “DW” = DEPTHWISE CONVOLUTIONS AND “NON-BT” = NOT BOTTLENECK STRUCTURE. THE INPUT AND OUTPUT ARE BOTH SIZE OF 64X64X128

Structures	FLOPs (M)	Parameters (K)
Bt	72.09	17.792
Bt+Fac	59.64	14.784
Bt+Dw	35.52	8.864
Bt+Fac+Dw	35.26	8.832
Non-bt	1209.01	295.424
Non-bt+Fac	807.40	197.120
Non-bt+Dw	145.75	36.096
Non-bt+Fac+Dw	143.65	35.840

#### 1) Down sampling block

Down sampling layers have both advantages and disadvantages. Down sampling layers enlarge the receptive field so that each pixel can get rich context information, and it also helps to save parameters that can reduce model size. But too much down sampling layers increases difficulty in recovering spatial information, especially harmful to dense classification tasks. Following the principle of ENet [20], our networks have three down sampling layers totally, the first two is performed at the forefront consecutively and another down sampling layer is after stage1, we adopted the initial block in ENet as our initial block and then replaced the standard convolution by depth-wise convolution used for the other two down sampler which is much weight-lighter than the original one (shown in Fig. 2(b)). Because the output of such down samplers is concatenation of two branches, we tried to refine the channel-wise independent features. Due to the great cost of using point-wise convolutions [17], we add channel shuffle at the end of down sampling blocks. But the accuracy decreases 2 points instead, so we do not use any additional combination operation after down sampling block in our final networks.

#### 2) Decoder choice

In encoder-decoder architectures, the encoder is used to extract high-level semantic features and the decoder is used to recover the output from encoder to original resolution. The existing works [9, 11] usually have heavy-weight decoder. Following the light-weight decoder view from ENet [20], We tried to shorter the decoder by evaluating different transposed convolutions with 2x, 4x and 8x up sampling rate, but we found that the bigger up sampling rate is, the worse prediction will be got. For the shortest decoder, we remove the decoder and use the bilinear interpolation to upsample the feature maps by a factor of 8 to the size of the original resolution, but there is about 3 points accuracy loss. In summary, in our decoder we use transposed convolution to perform upsample with factor of 2 and use SFRB to refine the feature maps which can be seen a better trade-off.

## IV. EXPERIMENTS

In this section, we first introduce the dataset and training environment used in our experiments, and then we design sets of ablation studies to demonstrate our model is high accuracy

and efficiency, finally we compare our models with the state-of-the-art networks and analyze the comparison results.

### A. General Setup

#### 1) WHU Building Dataset

We evaluated our methods on aerial imagery dataset from WHU Building Dataset which is a recent challenging dataset created by [18]. The aerial dataset consists of more than 22,000 independent buildings with different color, size and usage extracted from aerial images with 0.0075 m spatial resolution and 450  $km^2$  covering Christchurch, New Zealand which contains complex and various land cover feature and objects. The most parts of aerial images are downsampled to 0.3 m ground resolution and cropped into 8,189 non-overlapping tiles with  $512 \times 512$  pixels, these tiles make up the whole dataset. Then it was split into three parts, 4736 tiles for training, 1036 tiles for validation and 2416 tiles for testing. We train our model on the train dataset, validate it at the end of each epoch and then test the performance on test dataset. The metric we use to measure segmentation prediction is Intersection-over-Union (IoU) metric which is also called Jaccard Index and extensively adopted in segmentation tasks:

$$IoU = \frac{TP}{TP + TN + FP} \quad (11)$$

Where  $TP$ ,  $FP$  and  $FN$  are the number of true positives, false positives and false negatives pixels respectively.

#### 2) Training Configuration

All the experiments are implemented by Pytorch1.0.1. post2 with CUDA9.0 and CuDNN7. The models are trained on single Tesla V100 in 300 epochs, using Adam optimizer with weight decay of 0.0002 and momentum of 0.9. We set the initial learning rate to 0.0005 and use poly learning rate policy as many previous works, where the learning rate is multiplied by  $(1 - \text{iter} / \text{max\_iter})^{\text{power}}$  with power of 0.9. We set the batch size to 16 to fit our GPU memory. For fair comparisons, we adopted the weighted loss scheme defined as  $W_{\text{class}} = 1 / \log(P_{\text{class}} + c)$  followed by ENet [20] to mitigate the problem of unbalanced classes, where we set  $c$  to 1.12. The data augmentation strategies we used only include random horizontal flip and random vertical flip. The whole training phase is really fast, just needs 4 hours and low memory consumption.

### B. Ablation Studies

In this subsection, we conduct sets of experiments to demonstrate the accuracy and efficiency of our methods as shown in Table III. All the following results are based on test dataset in WHU Building Dataset.

#### 1) Core Modules

The separable factorized residual block is our core module, and the key-modules are depth-wise separable convolutions and factorized convolutions, so we designed another two variants of our network to further explain the efficiency of our modules. The first one is “non-depth-wise” variant which is bottleneck structure with factorized convolutions, replacing the

standard  $3 \times 3$  convolution into  $3 \times 1$  and  $1 \times 3$  convolutions in residual branch. The other one is “non-factorized” variant implemented by replacing the standard  $3 \times 3$  convolution into a depth-wise one without factorized kernels. For fair, we used the same backbone and training configuration to train these two

TABLE III  
THE LIST OF THE COMPARISON RESULTS OF ABLATION STUDIES AND ALL THE RESULTS ARE BASED ON TEST DATASET. THE NAMES OF NETWORKS ARE DECLARED IN SECTION IV-B

Networks	FLOPs (G)	Parameters (M)	IoU
ESFNet-base (ours)	2.514	0.1775	85.34
ESF-Bt	3.075	0.26	85.63
ESF-Bt-Fac	2.884	0.24	85.73
ESF-Bt-Dw	2.521	0.1779	85.75
ESF-NonBt	20.700	2.98	86.72
ESF-NonBt-Fac	14.486	2.02	86.93
ESF-NonBt-Dw	4.330	0.4495	86.93
ESF-NonBt-Fac-Dw	4.275	0.4465	85.54
ESF-ENet-down	2.744	0.22	85.56
ESF-improved-down	2.513	0.18	83.30
ESF-trans2x4x	2.112	0.17	50.58
ESF-trans8x	1.131	0.10	13.20
ESF-interp8x	0.527	0.09	82.12
ESF-mini	2.373	0.14	84.57
ESF-mini-ex	2.299	0.14	84.29

variants, and these two networks are named as ESF-Bt-Dw and ESF-Bt-Fac respectively.

As 2-8 lines in Table III demonstrates that, our ESFNet-base achieves no more than 1% accuracy loss compared with ESF-Bt-Fac and ESF-Bt-Dw. But the ESF-Bt-Fac has 11% more computational cost and 30% more parameters than our final model. The ESF-Bt-Dw is slightly more than ESFNet-base in FLOPs and the number of parameters, because the model is already small that the difference of  $3 \times M \times M \times C$  and  $3 \times C$  cannot be vast gaps as analyzing in Section III. It indicates that the depth-wise convolutions have more powerful performance than the factorized convolutions in improving network efficiency and further combining two approaches will get much better result. The similar accuracy shows that the more parameters do not mean more accuracy, and there are really much parameters and computation redundancies in deep neural networks which needed to solve urgently.

#### 2) Down Sampling Block

Following with ERFNet, we also adopted the initial block as our first down sampling block, and we further extended the initial block to two variants. The first variant, which is used in our final model, is implemented by replacing the standard  $3 \times 3$  convolution into depth-wise one. Another one designed for combining the channel-wise independent features as described in Section III-B, we added channel shuffle operation after the concatenation of main branch and pooling branch.

In order to investigate our efficient down sampling block, we compared ours with another two variants of ESFNet shown in 9-10 lines. The first variant named as ESF-ENet-down uses initial block in all down sampling layers like ERFNet. The second one named ESF-improved-down implemented by

adding channel shuffle operation after the concatenation at the end of down sampler. Similarly, our ESFNet-base achieves almost equal accuracy to ESF-ENet-down, but with 18% less parameters and 7% less FLOPs. The basic idea of ESF-improve-down is to combine the channel-wise independent features, but it has 2 points accuracy drop instead which might be caused by channel shuffle operation among unequal groups. So we did not adopt channel shuffle in ESFNet.

### 3) Light-weight Decoder

Encoder-decoder architecture is one of the most popular architecture in semantic segmentation tasks. The symmetric structure means that decoder is an exact mirror of the encoder which is deep and wide. In contrast, [20] provides a light-weight decoder view that the decoder only used for recovering the high-level feature maps to original resolution and fine-tuning. So we have an exploratory work about light-weight decoder for further studies, we performed comparisons on four variants of ESFNet with lighter and lighter decoder, they are ESFNet, ESFNet-trans2x4x, ESFNet-trans8x and ESFNet-interp8x where 2x, 4x and 8x means the upsampling rate of transposed convolutions and interp8x means that using bilinear interpolate with factor of 8 instead of decoder. The comparison results are reported in 11-13 lines. Though using transposed convolution with high upsampling rate like 4x and 8x brings much lighter decoder than the ESFNet-base, the accuracy drastically falls to 50.58% and 13.20% respectively. Transposed convolutions implement upsampling by inserting blanks between consecutive pixels in original feature maps similar to dilated convolutions and then performing standard convolution operation on the upsampled feature maps. So the bad performance of transposed convolution with high upsampling rate is due to inserting too much blanks that destroys the high-level feature representations extracted in encoder phase. The bilinear interpolate is a straight-forward method to recover original resolution, the prediction result of ESFNet-interp8x fits the view that the decoder is just for recovering and fine-tuning. The ESFNet-interp8x only requires 1/5 FLOPs and 1/2 parameters of ESFNet-base, but with 3 points drop in accuracy, it indicates the decoders in novel symmetric structures [9, 10, 11] is redundant and it is necessary to have light-weight decoder. For preserving better balance between accuracy and efficiency, we employed transposed convolution with upsampling rate of 2 and SFRB for fine-tuning in our network.

### 4) Mini-version

We extended our ESFNet-base to mini-versions according to the characteristics of ResNet. Veit *et al.* [42] proposed that dropping a single residual block only has a little influence on the accuracy, Greff *et al.* [43] said each residual in the same stage does not learn a new representation but learn an unrolled iterative estimation, in another word the following residual blocks is used to refine the coarse estimation from the first

block in each stage. Under the premise of enough receptive fields to cover the whole aerial images, we dropped four SFRB in stage2 whose dilation rate is equal to one, and consider this network as ESF-mini, in this case the receptive field is 535. Furthermore, we dropped two SFRB in stage1 and name it as ESF-mini-ex, and the receptive of ESF-mini-ex is 519 that is still enough to cover the whole image. On one hand there is too much redundancy information in early stage, on the other hand it makes the stage2 relatively close to the supervisions and lets it learn a better representation [44]. The ESF-mini and ESF-mini-ex have both have 22% less parameters and 8%, 12%

TABLE IV  
THE TABLE OF THE COMPARISON RESULT OF OUR ARCHITECTURE TO THE STATE-OF-THE-ART MODELS. ALL RESULTS ARE BASED ON TEST DATASET OF WHU BUILDING DATASET. “FLOPS” = FLOATING POINT OPERATIONS, “IOU” = INTERSECTION OVER UNION, “FPS” = FRAMES PER SECOND

Networks	FLOPs (G)	Parameters (M)	IoU	FPS
CU-Net	-	-	87.1	-
FCN	-	>130	85.4	-
SegNet	160.323	29.44	-	51.31
UNet	1238.811	13.40	86.8	-
SiU-Net	1238.811	13.40	88.4	-
ENet	2.215	0.36	86.03	48.08
ERFNet	14.674	2.06	87.03	88.24
EDANet	4.410	0.68	84.05	88.83
Ours-base	2.513	0.18	85.34	100.29
Ours-mini	2.372	0.14	84.57	119.89
Ours-mini-ex	2.299	0.14	84.29	142.98

fewer FLOPs compared to ESFNet-base and the accuracy loss just at around 1%. It is worth to note that ESF-mini-ex have significant improvement on inference speed, we will elaborate in the next part.

## V. EVALUATION

As shown in Table IV, we compared our ESFNet-base and its mini-versions with other state-of-the-art networks (i.e. SiU-Net, CU-Net, Unet and FCN which come from the original paper [29]) and novel real-time architectures (i.e. ENet [20], ERFNet [21] and EDANet [22] which are in similar structure and easy to deploy). All the comparison results are based on test dataset with the same training environment and configuration. The accuracy of networks is measured by IoU, and we used Frames Per Second (FPS) to measure the inference speed, and “-” means that this value is not given. The structure of CU-Net and FCN, is not given clearly in the original paper [29] and we do not display FLOPs, Params and FPS in table, but we know CU-Net has similar structure with UNet [11] and FCN-8s [8] already has over 130 M parameters, both of them are heavy-weight networks. Though SegNet [9] has much lighter decoder than other encoder-decoder architectures, it still has so many parameters of 29.44 M that we cannot train it on a single GPU with batch size of 16 and we do not display its IoU. In the following part we perform detailed analysis on the comparison results.

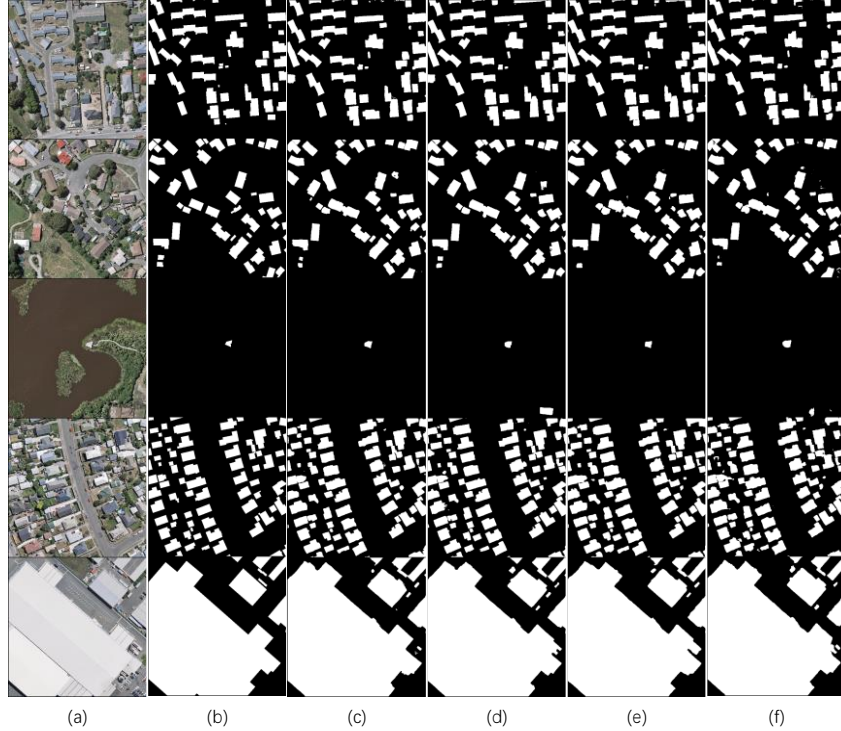


Fig. 3. Segmentation results of ENet (c), ERFNet (d), our ESFNet (e) and ESFNet-mini-ex (f). (a) Aerial image. (b) Ground Truth. All the images are randomly select from test dataset.

The results show that our ESFNet-base can achieve similar accuracy to the state-of-the-art and obtain much better trade-off between accuracy and efficiency than previous real-time networks. Our architecture ESFNet-base achieves 85.34% IoU on test dataset with 2.513 G FLOPs and 0.18 M parameters, it can perform 100.29 predictions per second and then we extended our ESFNet-base to ESF-mini-ex which has only 1 point accuracy drop but with lower FLOPs and less parameters than the base one, the ESFNet-mini-ex can run 142.98 FPS under the same experiment environment, the improvement is significant.

Most of previous networks for segmentation tasks are encoder-decoder architecture, by making networks deeper and wider or using additional scheme to achieve high accuracy, such as SegNet, SiU-Net, CU-Net and UNet, but these networks need high computational cost and resources. The top-accuracy method SiU-Net in Table IV, which uses the original U-Net with multi-resolution input scheme, achieve 88.4% IoU but it requires 13.40 M parameters and 1238.811 G FLOPs. Compared to the top-accuracy network, our ESFNet-base only has accuracy drop of 3 points and our network needs 74x less parameters and 492x lower FLOPs. Our ESFNet-base achieves similar accuracy to the FCN, but FCN has over 130 M parameters which is a huge number compared to 0.18 M. It demonstrates that there is large amount of redundancies in previous high-accuracy networks, and our networks can utilize parameters much more efficiently to learn the similar representation to the top-accuracy one. In summary, previous high-accuracy networks are not comparable to our networks and other real-time networks in efficiency, and the real-time network family can achieve better balance between accuracy and efficiency.

We compared our ESFNet to some of novel real-time networks, which both utilize residual learning. The ENet and ERFNet both benefits from ResNet architecture, ERFNet achieves much higher IoU 87.03% than ENet 86.03% but it can run 2x faster than ENet with higher FLOPs and larger model size in our experiment, it might because ENet partially uses decomposed convolutions and ERFNet fully uses. It proves the excellent performance of factorized convolutions both in accuracy and efficiency. EDANet has lower FLOPs and less parameters than ERFNet, it achieves 84.05% IoU but with similar inference speed to ERFNet, the reason is that dense blocks need much memory resources to save high resolution feature maps in intermediate layers which means high memory access cost, and the lower accuracy is caused by bilinear interpolate upsampling method analyzed in Section IV-B. Our ESFNet-base achieves 85.32% IoU on test dataset which is a slight drop and it can run 12 more frames per second than ERFNet. Our ESFNet-mini-ex highly improves the inference speed to 142.98 FPS while preserving acceptable accuracy of 84.29% IoU. Therefore, our core module SFRB and our network designation scheme significantly enhances the performance of networks for semantic segmentation tasks, both in accuracy and efficiency.

## VI. CONCLUSIONS

In this paper, we proposed novel efficient and accurate architecture ESFNet for building extraction task. Different from the previous state-of-the-art networks, our networks can achieve similar accuracy with lower computational cost and less parameters. Our ESFNet-base achieves 85.34% IoU and 100.29 FPS on WHU Building Dataset, and our ESFNet-mini-ex achieves 84.29% IoU and 142.98 FPS. We

designed a highly efficient module SFRB as our core module based on residual block which can be deployed in most of existing architectures, and we analyzed the efficient and accurate network designation scheme for semantic segmentation networks. Through comprehensive ablation studies and sets of comparisons with top-accuracy and top-fast networks, it indicates that our ESFNet can provide a better trade-off between accuracy and speed which makes remote sensing researches much more efficient.

## REFERENCES

- [1] R. Li et al., "DeepUNet: A Deep Fully Convolutional Network for Pixel-level Sea-Land Segmentation," arXiv:1709.00201 [cs], Sep. 2017.
- [2] G. Cheng, Y. Wang, S. Xu, H. Wang, S. Xiang, and C. Pan, "Automatic Road Detection and Centerline Extraction via Cascaded End-to-End Convolutional Neural Network," *IEEE Transactions on Geoscience and Remote Sensing*, vol. 55, no. 6, pp. 3322–3337, Jun. 2017.
- [3] G. Cheng, C. Ma, P. Zhou, X. Yao, and J. Han, "Scene classification of high resolution remote sensing images using convolutional neural networks," in *2016 IEEE International Geoscience and Remote Sensing Symposium (IGARSS)*, 2016, pp. 767–770.
- [4] Y. Xu, L. Wu, Z. Xie, and Z. Chen, "Building Extraction in Very High Resolution Remote Sensing Imagery Using Deep Learning and Guided Filters," *Remote Sensing*, vol. 10, no. 1, p. 144, Jan. 2018.
- [5] A. Krizhevsky, I. Sutskever, and G. E. Hinton, "ImageNet Classification with Deep Convolutional Neural Networks," in *Advances in Neural Information Processing Systems 25*, F. Pereira, C. J. C. Burges, L. Bottou, and K. Q. Weinberger, Eds. Curran Associates, Inc., 2012, pp. 1097–1105.
- [6] T.-Y. Lin et al., "Microsoft COCO: Common Objects in Context," arXiv:1405.0312 [cs], May 2014.
- [7] M. Everingham, L. Van Gool, C. K. I. Williams, J. Winn, and A. Zisserman, "The Pascal Visual Object Classes (VOC) Challenge," *International Journal of Computer Vision*, vol. 88, no. 2, pp. 303–338, Jun. 2010.
- [8] J. Long, E. Shelhamer, and T. Darrell, "Fully Convolutional Networks for Semantic Segmentation," p. 10.
- [9] V. Badrinarayanan, A. Kendall, and R. Cipolla, "SegNet: A Deep Convolutional Encoder-Decoder Architecture for Image Segmentation," arXiv:1511.00561 [cs], Nov. 2015.
- [10] H. Noh, S. Hong, and B. Han, "Learning Deconvolution Network for Semantic Segmentation," arXiv:1505.04366 [cs], May 2015.
- [11] O. Ronneberger, P. Fischer, and T. Brox, "U-Net: Convolutional Networks for Biomedical Image Segmentation," arXiv:1505.04597 [cs], May 2015.
- [12] L.-C. Chen, G. Papandreou, I. Kokkinos, K. Murphy, and A. L. Yuille, "Semantic Image Segmentation with Deep Convolutional Nets and Fully Connected CRFs," arXiv:1412.7062 [cs], Dec. 2014.
- [13] L.-C. Chen, G. Papandreou, I. Kokkinos, K. Murphy, and A. L. Yuille, "DeepLab: Semantic Image Segmentation with Deep Convolutional Nets, Atrous Convolution, and Fully Connected CRFs," arXiv:1606.00915 [cs], Jun. 2016.
- [14] L.-C. Chen, G. Papandreou, F. Schroff, and H. Adam, "Rethinking Atrous Convolution for Semantic Image Segmentation," arXiv:1706.05587 [cs], Jun. 2017.
- [15] L.-C. Chen, Y. Zhu, G. Papandreou, F. Schroff, and H. Adam, "Encoder-Decoder with Atrous Separable Convolution for Semantic Image Segmentation," arXiv:1802.02611 [cs], Feb. 2018.
- [16] N. Ma, X. Zhang, H.-T. Zheng, and J. Sun, "ShuffleNet V2: Practical Guidelines for Efficient CNN Architecture Design," arXiv:1807.11164 [cs], Jul. 2018.
- [17] A. G. Howard et al., "MobileNets: Efficient Convolutional Neural Networks for Mobile Vision Applications," arXiv:1704.04861 [cs], Apr. 2017.
- [18] M. Sandler, A. Howard, M. Zhu, A. Zhmoginov, and L.-C. Chen, "MobileNetV2: Inverted Residuals and Linear Bottlenecks," arXiv:1801.04381 [cs], Jan. 2018.
- [19] X. Zhang, X. Zhou, M. Lin, and J. Sun, "ShuffleNet: An Extremely Efficient Convolutional Neural Network for Mobile Devices," arXiv:1707.01083 [cs], Jul. 2017.
- [20] A. Paszke, A. Chaurasia, S. Kim, and E. Culurciello, "ENet: A Deep Neural Network Architecture for Real-Time Semantic Segmentation," arXiv:1606.02147 [cs], Jun. 2016.
- [21] E. Romera, J. M. Alvarez, L. M. Bergasa, and R. Arroyo, "ERFNet: Efficient Residual Factorized ConvNet for Real-Time Semantic Segmentation," *IEEE Transactions on Intelligent Transportation Systems*, vol. 19, no. 1, pp. 263–272, Jan. 2018.
- [22] S.-Y. Lo, H.-M. Hang, S.-W. Chan, and J.-J. Lin, "Efficient Dense Modules of Asymmetric Convolution for Real-Time Semantic Segmentation," arXiv:1809.06323 [cs], Sep. 2018.
- [23] K. He, X. Zhang, S. Ren, and J. Sun, "Deep Residual Learning for Image Recognition," arXiv:1512.03385 [cs], Dec. 2015.
- [24] E. Maggiori, Y. Tarabalka, G. Charpiat, and P. Alliez, "Convolutional Neural Networks for Large-Scale Remote-Sensing Image Classification," *IEEE Transactions on Geoscience and Remote Sensing*, vol. 55, no. 2, pp. 645–657, Feb. 2017.
- [25] K. Simonyan and A. Zisserman, "Very Deep Convolutional Networks for Large-Scale Image Recognition," arXiv:1409.1556 [cs], Sep. 2014.
- [26] J. Yuan, "Learning Building Extraction in Aerial Scenes with Convolutional Networks," *IEEE Transactions on Pattern Analysis and Machine Intelligence*, vol. 40, no. 11, pp. 2793–2798, Nov. 2018.
- [27] L. Li, J. Liang, M. Weng, and H. Zhu, "A Multiple-Feature Reuse Network to Extract Buildings from Remote Sensing Imagery," *Remote Sensing*, vol. 10, no. 9, p. 1350, Sep. 2018.
- [28] G. Huang, Z. Liu, L. van der Maaten, and K. Q. Weinberger, "Densely Connected Convolutional Networks," arXiv:1608.06993 [cs], Aug. 2016.

[29] S. Ji, S. Wei, and M. Lu, “Fully Convolutional Networks for Multisource Building Extraction From an Open Aerial and Satellite Imagery Data Set,” *IEEE Transactions on Geoscience and Remote Sensing*, vol. 57, no. 1, pp. 574–586, Jan. 2019.

[30] C. Yu, J. Wang, C. Peng, C. Gao, G. Yu, and N. Sang, “BiSeNet: Bilateral Segmentation Network for Real-time Semantic Segmentation,” arXiv:1808.00897 [cs], Aug. 2018.

[31] H. Zhao, X. Qi, X. Shen, J. Shi, and J. Jia, “ICNet for Real-Time Semantic Segmentation on High-Resolution Images,” arXiv:1704.08545 [cs], Apr. 2017.

[32] T. Zhang, G.-J. Qi, B. Xiao, and J. Wang, “Interleaved Group Convolutions for Deep Neural Networks,” arXiv:1707.02725 [cs], Jul. 2017.

[33] J. Alvarez and L. Petersson, “DecomposeMe: Simplifying ConvNets for End-to-End Learning,” arXiv:1606.05426 [cs], Jun. 2016.

[34] P. Wang et al., “Understanding Convolution for Semantic Segmentation,” arXiv:1702.08502 [cs], Feb. 2017.

[35] H. Zhao, J. Shi, X. Qi, X. Wang, and J. Jia, “Pyramid Scene Parsing Network,” arXiv:1612.01105 [cs], Dec. 2016.

[36] R. Hamaguchi, A. Fujita, K. Nemoto, T. Imaizumi, and S. Hikosaka, “Effective Use of Dilated Convolutions for Segmenting Small Object Instances in Remote Sensing Imagery,” Sep. 2017.6.

[37] S. Jégou, M. Drozdzal, D. Vazquez, A. Romero, and Y. Bengio, “The One Hundred Layers Tiramisu: Fully Convolutional DenseNets for Semantic Segmentation,” arXiv:1611.09326 [cs], Nov. 2016.

[38] S. Zagoruyko and N. Komodakis, “Wide Residual Networks,” arXiv:1605.07146 [cs], May 2016.

[39] S. Ioffe and C. Szegedy, “Batch Normalization: Accelerating Deep Network Training by Reducing Internal Covariate Shift,” Feb. 2015.

[40] X. Glorot, A. Bordes, and Y. Bengio, “Deep Sparse Rectifier Neural Networks,” in *Proceedings of the Fourteenth International Conference on Artificial Intelligence and Statistics*, 2011, pp. 315–323.

[41] F. Chollet, “Xception: Deep Learning with Depthwise Separable Convolutions,” Oct. 2016.

[42] A. Veit, M. Wilber, and S. Belongie, “Residual Networks Behave Like Ensembles of Relatively Shallow Networks,” May 2016.

[43] K. Greff, R. K. Srivastava, and J. Schmidhuber, “Highway and Residual Networks learn Unrolled Iterative Estimation,” arXiv:1612.07771 [cs], Dec. 2016.

[44] Z. Zhang, X. Zhang, C. Peng, D. Cheng, and J. Sun, “ExFuse: Enhancing Feature Fusion for Semantic Segmentation,” arXiv:1804.03821 [cs], Apr. 2018.